THE ASTRONOMICAL JOURNAL, 119:2403–2414, 2000 May

BINARY STAR DIFFERENTIAL PHOTOMETRY USING THE ADAPTIVE OPTICS SYSTEM AT MOUNT WILSON OBSERVATORY[1]

THEO TEN BRUMMELAAR[2]
Center for High Angular Resolution Astronomy, Georgia State University, Atlanta, GA 30303-3083; theo@mtwilson.edu
BRIAN D. MASON
US Naval Observatory, 3450 Massachusetts Avenue, NW, Washington, DC 20392-5420; bdm@draco.usno.navy.mil
AND
HAROLD A. MCALISTER,[2] LEWIS C. ROBERTS, JR.,[2,3] NILS H. TURNER,[2,4] WILLIAM I. HARTKOPF,[2,5]
AND WILLIAM G. BAGNUOLO, JR.[2]
Center for High Angular Resolution Astronomy, Georgia State University, Atlanta, GA 30303-3083; hal@chara.gsu.edu,
lroberts@cygnus.mhpcc.af.mil, nils@mtwilson.edu, hartkopf@chara.gsu.edu, bagnuolo@chara.gsu.edu
Received 1999 September 13; accepted 2000 January 31

ABSTRACT

We present photometric and astrometric results for 36 binary systems observed with the natural guide star adaptive optics system of the Mount Wilson Institute on the 100 inch (2.5 m) Hooker Telescope. The measurements consist of differential photometry in *U*, *B*, *V*, *R*, and *I* filters along with astrometry of the relative positions of system components. Magnitude differences were combined with absolute photometry found in the literature of the combined light for systems to obtain apparent magnitudes for the individual components at standard bandpasses, which in turn led to color determinations and spectral types. The combination of these results with *Hipparcos* parallax measurements yielded absolute magnitudes and allowed us to plot the components on an H-R diagram. To further examine the reliability and self-consistency of these data, we also estimated system masses from the spectral types.

Key words: binaries: general — binaries: visual — instrumentation: adaptive optics — techniques: photometric

1. INTRODUCTION

While the study of binary star systems is a very mature science, there are relatively few systems for which the temperatures and luminosities of the individual components are known. The Center for High Angular Resolution Astronomy (CHARA), at Georgia State University, has been using speckle interferometry for over 20 years to study multiple-star systems, and this technique has proved very productive for astrometry. Unfortunately, it has been much less effective in yielding photometric results. For close binary systems it is extremely challenging to obtain accurate photometric measurements of the individual components using standard techniques because, except in exceptional seeing conditions, the images of the two stars overlap. One exception to this statement is the analysis of the Capella system by Bagnuolo & Sowell (1988).

However, adaptive optics makes it feasible to directly measure magnitude differences and then, by combining these data with photometry of the system as a whole, obtain apparent magnitudes of the individual components. If this is done in a number of filters, colors can be calculated and effective temperatures derived through color-temperature relations. These data can then be combined with parallax measurements to place the stars on an H-R diagram.

In 1996 and 1997, CHARA received funding from the National Science Foundation and the Mount Wilson Institute (MWI) to pursue these measurements using the natural guide star adaptive optics (AO) system developed by MWI (Shelton et al. 1995) on the 100 inch (2.5 m) Hooker Telescope. In all, some 36 systems were measured in two or more filters on the Johnson et al. (1966) system. These results are presented below.

2. OBSERVATIONAL AND DATA REDUCTION TECHNIQUES

The strategy for observation and data reduction was a modification of the methods in our previous work at the Starfire Optical Range (SOR) by ten Brummelaar et al. (1996). A relatively short exposure time was chosen, such that the image was not saturated but the signal was well above the bias levels of the CCD camera. Between 10 and 50 exposures were taken of the object and then integrated into a composite image using a shift-and-add algorithm in which the Strehl ratio serves as a weight for each frame.

We then assume that the image consists of a series of functions of the form

$$\delta(x, y) = \begin{cases} 1, & \text{for } (x, y) = (0, 0), \\ 0, & \text{otherwise}. \end{cases} \quad (1)$$

So if the intensity of the ith star is A_i and its position is (x_i, y_i), the "clean" image can be written

$$I(x, y) = \sum_{i=1}^{N} A_i \, \delta(x - x_i, y - y_i) . \quad (2)$$

[1] Based on observations made at Mount Wilson Observatory, operated by the Mount Wilson Institute under an agreement with the Carnegie Institution of Washington.
[2] Visiting Astronomer, Mount Wilson Observatory, operated by the Mount Wilson Institute.
[3] Current address: Rocketdyne Technical Services, Suite 200, 535 Lipoa Parkway, Kihei, HI 96753.
[4] Current address: Mount Wilson Institute, P.O. Box 60947, Pasadena, CA 91023.
[5] Current address: US Naval Observatory, 3450 Massachusetts Avenue, NW, Washington, DC 20392-5420.

This image must then be convolved with the point-spread function (PSF) $P(x, y)$ to yield the "dirty" image

$$O(x, y) = I(x, y) * P(x, y) , \quad (3)$$

where we assume that the PSF does not change over the small 2″ field.

Given a pixel-by-pixel model of the PSF, which in the first instance can be provided by an image of a single star, one can then solve, in a least-squares sense, for the positions and magnitudes of the stars in the field. Of course, it is well known that an image of a single star does not make a very good PSF model, since both the performance of the AO system and the atmosphere itself will change substantially between observations. Thus, with these estimates of position and magnitude one extracts a new model of the PSF from the data themselves, using

$$P_k(x, y) = O(x, y) - \sum_{j \neq i} A_j[\delta(x - x_j, y - y_j) * P_{k-1}(x, y)] , \quad (4)$$

which can be done for each star in the field, and a mean, weighted by magnitude, created. This is a new PSF model and the process can be repeated until the results converge.

There are two areas in which our current techniques differ from those used in our earlier SOR work. The first is in the way we prevent the solution from converging to a single delta function and a multiple PSF model, which is a mathematically valid solution but not a useful one. Unless we are very close to convergence, the PSF model often contains some energy at the positions of the fainter stars in the field. In our previous work we forced the PSF model to exist only within a predefined boundary and to be zero elsewhere. This method ignores the often large amount of energy in the PSF wings. Instead of forcing the wings to zero, we now force the PSF to be circularly symmetric in the wings. Thus the PSF model has a nonanalytical part consisting of a matrix of numbers near the center, and a series of single values for various distances from the center. We found that a crossover point based on the first estimate of magnitude distance worked well, that is,

$$r_{\text{cross}} = \sqrt{(x_1 - x_2)^2 + (y_1 - y_2)^2}\, \frac{A_1}{A_1 + A_2} . \quad (5)$$

In some cases it was necessary to manually manipulate this crossover point in order to find the solution with the lowest residuals.

The second way in which we have changed our reduction method is in the area of error estimation. We now believe that the errors of the original work at SOR were underestimated and represent a lower bound on the errors. This is because those errors were based directly on the formal errors that came out of the least-squares fitting process. Since this is only valid if the functional form of the PSF is known exactly, which can never truly be the case, this will not be a true representation of the errors of the results. Simply using the formal error of the fit does not include the errors in the PSF model itself.

We now base our errors on a series of experiments in which we created a large pool of simulated data of known separation and magnitude difference and applied our reduction software to these images. We collected data on some 74 stars, known to be single within the resolving power of the telescope, in exactly the same way as we did for the binary systems. We then normalized these images to form PSF models and used equations (2) and (3) to create an ensemble of model binary star images ranging from 0 to 7 in magnitude difference and up to 2″ in separation. All in all, this represented a pool of over 30,000 model images. We then ran our reduction software on these data.

The resulting errors are a function of the magnitude difference and the separation, expressed in terms of the FWHM of the PSF. We found that one could reach the 10% level at small separations (a few FWHMs) down to a magnitude difference of 2, while if the stars are well separated one can reach 5.5 mag. The 1% error level can reach as deep as 3 mag, while one can go as deep as 7.5 mag at the 15% level. The errors are a strong function of how well the AO system is performing, which is in turn a function of the current seeing conditions. Since we did not have the luxury of working only in good seeing, which was on occasion in excess of 2″, we were forced to use what data we could collect. If the AO system is performing at the diffraction limit, which is not always the case in the V and B bands, one is often operating in the 1% to 2% regime. At other times the errors will be larger, depending on the FWHM yielded by the system. One would expect much smaller errors in an infrared AO system.

This method of estimating errors is much more conservative than those used in the past, including by us, as it does more than quote the formal error of the least-squares fitting process. We believe it to be closer to an upper bound. This should be taken into account when comparing the results from the two sets of measurements. These methods are more fully described by ten Brummelaar et al. (1998) and Roberts (1998).

The deconvolution routine provided a measurement of the differential magnitude of the two stars along with differential astrometric results, which we transform into the standard (θ, ρ) system for binary star measurements. The astrometry was calibrated with contemporaneous speckle interferometry measurements obtained on the 100 inch telescope (Hartkopf et al. 2000). The results are given in Tables 1 and 2. In Table 1, the first five columns give various identifications: the Washington Double Star Catalog (WDS) coordinate (Worley & Douglass 1997),[6] the discovery designation (as defined in the WDS), HR and HD numbers, and the Bayer or Flamsteed designation. For subsequent tables only the WDS coordinate is used, so Table 1 also serves as a cross-reference for the other tables. Columns (6)–(8) of Table 1 provide the basic calibrated astrometric data: time (expressed in fractional Besselian year), position angle θ (measured for the secondary relative to the primary from north to east in degrees), and angular separation ρ (in arcseconds). The last three columns in Table 1 give residuals to the orbit referenced in the final column.

While astrometry was not the primary objective in obtaining these data (speckle interferometric techniques provide more accurate and more straightforward measurements of θ and ρ), the astrometric results do provide a good check on the orbital parameters of these systems. However, in comparison with the autocorrelation methods commonly

[6] See http://aries.usno.navy.mil/ad/wds/wdsold.html.

TABLE 1

ADAPTIVE OPTICS ASTROMETRY

WDS α, δ (2000) (1)	Discovery Designation (2)			HR (3)	HD (4)	Name (5)	BY (1990.0+) (6)	θ (deg) (7)	ρ (arcsec) (8)	$\Delta\theta$ (deg) (9)	$\Delta\rho$ (arcsec) (10)	Orbit Ref. (11)
00022+2705.....	Bu	733	AB	9088	224930	85 Peg	6.7842	151	0.76	−1	+0.02	1
00318+5431.....	Stt	12		123	2772	λ Cas	6.7843	194	0.42	+0	−0.04	2
02140+4729.....	StF	228		647	13594	...	6.7845	280	1.03	+1	−0.01	3
04139+0916.....	Bu	547	AB	1311	26722	47 Tau	6.7818	342	1.24	...	...	
04239+0928.....	Hu	304		1381	27820	66 Tau	6.7900	335	0.11	+8	−0.01	4
04301+1538.....	StF	554		1422	28485	80 Tau	6.7847	18	1.61	+1	−0.12	5
							6.7901	17	1.63	+0	−0.10	
04382−1418.....	Kui	18		1481	29503	53 Eri	6.7847	350	0.92	+0	−0.05	6
04512+1104.....	Bu	883	AB	...	30810	...	6.7901	225	0.27	−1 r	−0.01	7
05387−0236.....	Bu	1032	AB	1931	37468	σ Ori	6.7901	121	0.26	+1	+0.01	6
05413+1632.....	Bu	1007		1946	37711	126 Tau	6.7902	244	0.29	+2	−0.01	8
06573+5825.....	Stt	159	AB	2560	50522	15 Lyn	6.7902	216	0.30	−10	−0.02	9
09006+4147.....	Kui	37	AB	3579	76943	...	7.2820	89	0.43	+1	+0.00	6
11182+3132.....	StF	1523	AB	4374/5	98230/1	ξ UMa	7.2794	291	1.54	−2	+0.01	10
							7.2823	291	1.52	−2	−0.01	
13099−0532.....	McA	38	Aa	4963	114330	θ Vir	6.5019	336	0.45	...	...	
13100+1732.....	StF	1728	AB	4968/9	114378/9	α Com	6.5019	192	0.33	+0 r	+0.00	6
14411+1344.....	StF	1865	AB	5477/8	129246/7	ζ Boo	6.4992	122	0.82	+1 r	−0.05	11
							7.2826	121	0.83	+0 r	−0.02	
15038+4739.....	StF	1909		5618	133640	44 Boo	7.2798	50	1.97	−2	−0.09	12
15183+2650.....	StF	1932	Aa-B	...	136176	...	7.6052	256	1.56	−2	−0.03	13
15232+3017.....	StF	1937	AB	5727/8	137107/8	η CrB	6.4965	47	0.90	+0	−0.01	14
							7.6025	51	0.87	−1	+0.01	
15427+2618.....	StF	1967		5849	140436	γ CrB	6.4965	117	0.68	+1	−0.01	15
							7.2828	113	0.71	−2	+0.00	
16309+0159.....	StF	2055	AB	6149	148857	λ Oph	6.4939	26	1.37	−1	−0.15	16
							7.2830	24	1.39	−4	−0.13	
17104−1544.....	Bu	1118	AB	6378	155125	η Oph	6.4967	245	0.51	+0	−0.01	17
							6.5021	246	0.51	+1	−0.01	
19307+2758.....	McA	55	Aa	7417	183915	β^1 Cyg	6.4995	139	0.39	...	...	
19553−0644.....	StF	2597		7599	188405	...	6.4996	105	0.38	+0	+0.00	6
							7.6001	117	0.37	+12	−0.04	
20035+3601.....	StF	2624	Aa-B	...	190429	...	6.4997	174	1.95	...	...	
20181+4044.....	StF	2666	Aa-B	7767	193322	...	6.4970	245	2.71	...	...	
20203+3924.....	A	1427	AB	7784	193702	...	6.4970	117	0.34	+1	+0.03	18
20375+1436.....	Bu	151	AB	7882	196524	β Del	6.4942	315	0.32	+0	+0.02	15
							6.4998	317	0.32	+2	+0.02	
21044−1951.....	Fin	328		8060	200499	η Cap	6.4998	236	0.26	+1 r	−0.01	14
21145+1000.....	Stt	535	AB	8123	202275	δ Equ	6.4944	20	0.27	+1	+0.00	6
21148+3803.....	AGC	13	AB	8130	202444	τ Cyg	6.4944	327	0.80	−2	+0.03	19
21186+1134.....	Bu	163	AB	...	202908	...	6.4999	262	0.42	+0	−0.02	20
21441+2845.....	StF	2822	AB	8309	206826/7	μ Cyg	6.7811	305	1.92	+1	+0.02	2
21501+1717.....	Cou	14		8344	207652	13 Peg	6.4945	233	0.38	−1	+0.00	15
22300+0426.....	StF	2912		8566	213235	37 Peg	6.4945	116	0.48	−2	−0.02	21
22586+0921.....	Stt	536	AB	8737	217166	...	6.4972	349	0.19	+2	−0.12	22

REFERENCES.—(1) Hall 1949; (2) Heintz 1995; (3) Heintz 1984; (4) Starikova 1985; (5) Baize 1980; (6) Hartkopf, Mason, & McAlister 1996; (7) Heintz 1969; (8) Docobo & Ling 1999; (9) Baize 1993; (10) Mason et al. 1995; (11) Wierzbinski 1956; (12) Heintz 1997; (13) Heintz 1965; (14) Mason, Douglass, & Hartkopf 1999; (15) Hartkopf, McAlister, & Franz 1989; (16) Finzi & Giannuzzi 1955; (17) Docobo & Ling 1997; (18) Docobo & Costa 1987; (19) Heintz 1970; (20) Fekel et al. 1997; (21) Zulević 1988; (22) Cester 1991.

used with speckle interferometry, AO yields a direct image of a system. Thus, the 180° uncertainty in position angle, inherent in earlier reductions of speckle interferometric data, is avoided. While current reduction techniques (i.e., the DVA algorithm; see Bagnuolo et al. 1992) can avoid this ambiguity, AO is more sensitive to very small magnitude differences. In the case of four systems, the correct quadrant identification indicated the published orbital analyses had the longitude of periastron (ω) off by 180°. Those systems are flagged with the letter "r" adjacent to the $\Delta\theta$ residual in column (9) of Table 1. In all cases, the determined astrophysical parameters of these systems are unchanged by the alteration of ω. In large-angle astrometry, the photocenter of these systems (which would probably be unresolved) would be determined for the wrong quadrant, leading to a position error. In three of these cases, the small Δm was responsible for the incorrect assignment of ω, and any consequential photocenter shift would be negligible. In the case of Fin 328 an incorrect quadrant was assigned by speckle interferometry, leading to the error (the quadrant was identified correctly by Finsen 1956 and noted by Söderhjelm 1999).

Table 2 provides the raw differential photometry for each observation. The first column lists the WDS coordinate, while the next column provides the date of observation. The remaining columns give the differential magnitude and error estimate for each system in the indicated passband. Most objects have magnitude differences in three to four passbands. Only one observation provides all five colors, while two observations provide only two colors.

The *U* and *B* filters were not always available, and in some cases the deconvolution did not converge. These factors result in the omissions from Table 2. In other cases, we measured an object twice at different epochs in order to test the consistency of the methods used. Except in the shorter wavelengths where the performance of the AO system was poor, these data are entirely self-consistent, giving us confidence in the results. Even in the bluer bands the multiple measurements are very close and, at worst, indicate that our error bars are underestimated in this band.

In order to evaluate the quality of our measurements, a literature search was done to find existing Δm values, which we present in Table 3. In this table, the same WDS coordinate identification is used. The literature sources of Δm are the *Hipparcos* Catalogue (ESA 1997), the WDS, and the internal US Naval Observatory (USNO) Δm catalog. Many double star lists do not provide true measures of Δm but simply repeat values from other catalogs. Consequently, the WDS Δm provides only a gross estimate and should be given the lowest weight. The USNO Δm catalog was initially assembled by C. Worley to include only those measures of differential magnitude known to be original. The

TABLE 2

ADAPTIVE OPTICS DIFFERENTIAL PHOTOMETRY

WDS α, δ (2000)	BY (1990.0+)	Δm				
		U	*B*	*V*	*R*	*I*
00022+2705	6.7842	...	...	3.08 ± 0.29	2.70 ± 0.27	2.35 ± 0.26
00318+5431	6.7843	...	...	0.15 ± 0.04	0.10 ± 0.04	0.13 ± 0.04
02140+4729	6.7845	...	...	0.65 ± 0.06	0.59 ± 0.04	0.54 ± 0.02
04139+0916	6.7818	...	...	2.43 ± 0.04	2.86 ± 0.07	3.28 ± 0.13
04239+0928	6.7900	...	...	0.90 ± 0.12	0.97 ± 0.11	0.21 ± 0.04
04301+1538	6.7847	...	...	2.35 ± 0.20	2.19 ± 0.17	2.02 ± 0.12
	6.7901	...	...	2.54 ± 0.07	2.37 ± 0.05	2.21 ± 0.03
04382−1418	6.7847	...	...	...	2.39 ± 0.23	3.02 ± 0.20
04512+1104	6.7901	...	...	0.15 ± 0.04	0.18 ± 0.04	0.20 ± 0.04
05387−0236	6.7901	...	...	1.24 ± 0.10	1.34 ± 0.13	1.25 ± 0.15
05413+1632	6.7902	...	...	1.47 ± 0.16	1.51 ± 0.18	1.52 ± 0.18
06573+5825	6.7902	...	...	1.16 ± 0.11	1.41 ± 0.08	1.60 ± 0.18
09006+4147	7.2820	2.11 ± 0.22	...	2.55 ± 0.27	2.19 ± 0.15	2.06 ± 0.23
11182+3132	7.2794	...	0.62 ± 0.08	0.53 ± 0.09	0.47 ± 0.06	0.40 ± 0.04
	7.2823	...	0.47 ± 0.05	0.42 ± 0.06	0.28 ± 0.06	0.18 ± 0.04
13099−0532	6.5019	...	2.11 ± 0.23	2.21 ± 0.20	2.08 ± 0.20	2.16 ± 0.21
13100+1732	6.5019	...	0.04 ± 0.04	−0.01 ± 0.06	0.00 ± 0.04	0.00 ± 0.03
14411+1344	6.4992	...	−0.00 ± 0.02	0.02 ± 0.01	0.01 ± 0.01	0.02 ± 0.01
	7.2826	0.06 ± 0.02	−0.02 ± 0.09	0.07 ± 0.04	0.01 ± 0.03	0.05 ± 0.03
15038+4739	7.2798	...	1.28 ± 0.16	0.82 ± 0.07	0.61 ± 0.03	0.52 ± 0.04
15183+2650	7.6052	...	0.02 ± 0.04	0.01 ± 0.03	0.00 ± 0.04	−0.03 ± 0.10
15232+3017	6.4965	...	0.32 ± 0.02	0.28 ± 0.02	0.26 ± 0.01	0.25 ± 0.01
	7.6025	...	0.36 ± 0.06	0.29 ± 0.06	0.28 ± 0.04	0.25 ± 0.04
15427+2618	6.4965	...	1.69 ± 0.08	1.56 ± 0.02	1.43 ± 0.02	1.33 ± 0.03
	7.2828	...	1.85 ± 0.11	1.59 ± 0.12	1.41 ± 0.06	1.28 ± 0.06
16309+0159	6.4939	...	...	1.07 ± 0.14	1.03 ± 0.04	1.02 ± 0.03
	7.2830	...	1.12 ± 0.07	1.11 ± 0.05	1.09 ± 0.05	1.06 ± 0.03
17104−1544	6.4967	...	0.50 ± 0.06	0.52 ± 0.04	0.53 ± 0.03	0.53 ± 0.02
	6.5021	...	0.54 ± 0.08	0.42 ± 0.05	0.47 ± 0.02	0.49 ± 0.01
19307+2758	6.4995	...	...	2.64 ± 0.19	3.47 ± 0.26	...
19553−0644	6.4996	...	1.22 ± 0.10	1.18 ± 0.12	1.10 ± 0.10	1.16 ± 0.06
	7.6001	...	0.28 ± 0.06	0.88 ± 0.12	1.00 ± 0.11	1.15 ± 0.13
20035+3601	6.4997	...	0.79 ± 0.04	0.76 ± 0.02	0.75 ± 0.01	0.74 ± 0.01
20181+4044	6.4970	...	2.72 ± 0.07	2.29 ± 0.04	2.31 ± 0.02	2.31 ± 0.01
20203+3924	6.4970	...	2.07 ± 0.22	1.96 ± 0.18	2.01 ± 0.22	1.68 ± 0.19
20375+1436	6.4942	...	1.25 ± 0.14	0.89 ± 0.11	0.93 ± 0.11	1.07 ± 0.14
	6.4998	...	0.84 ± 0.05	0.97 ± 0.06	1.03 ± 0.08	0.83 ± 0.09
21044−1951	6.4998	...	2.67 ± 0.26	2.18 ± 0.22	2.03 ± 0.21	1.72 ± 0.18
21145+1000	6.4944	...	0.19 ± 0.04	0.09 ± 0.04	0.09 ± 0.04	0.43 ± 0.05
21148+3803	6.4944	...	2.80 ± 0.22	2.74 ± 0.12	2.62 ± 0.09	2.59 ± 0.10
21186+1134	6.4999	...	1.68 ± 0.18	1.62 ± 0.14	1.53 ± 0.17	1.57 ± 0.14
21441+2845	6.7811	...	1.47 ± 0.03	...	1.41 ± 0.02	1.38 ± 0.01
21501+1717	6.4945	...	1.21 ± 0.14	1.25 ± 0.09	1.11 ± 0.09	1.08 ± 0.06
22300+0426	6.4945	...	2.01 ± 0.22	1.78 ± 0.20	1.54 ± 0.15	1.42 ± 0.12
22586+0921	6.4972	...	0.22 ± 0.04	1.62 ± 0.19	0.50 ± 0.08	−0.39 ± 0.83

TABLE 3

LITERATURE Δm VALUES

WDS α, δ (2000)	*Hipparcos*	Mean WDS	Δm Catalog
00022+2705	...	3.60 ± 1.19	3.04
00318+5431	0.04 ± 0.01	0.25 ± 0.17	...
02140+4729	0.66 ± 0.01	0.72 ± 0.21	0.57 ± 0.09
04139+0916	2.25 ± 0.04	2.68 ± 0.48	2.18
04239+0928	...	0.07 ± 0.09	...
04301+1538	2.52 ± 0.03	2.42 ± 0.54	2.38 ± 0.06
04382−1418	2.90 ± 0.02	2.99 ± 0.34	3.43
04512+1104	0.24 ± 0.20	0.12 ± 0.23	0.19
05387−0236	1.21 ± 0.05	1.15 ± 0.53	...
05413+1632	1.51 ± 0.04	0.65 ± 0.38	2.0
06573+5825	...	1.19 ± 0.48	1.20
09006+4147	2.30 ± 0.04	2.14 ± 0.35	1.83 ± 0.08
11182+3132	...	0.53 ± 0.24	0.48 ± 0.03
13099−0532	2.34 ± 0.04	...	...
13100+1732	...	0.05 ± 0.08	0.41 ± 0.51
14411+1344	0.05 ± 0.01	0.52 ± 0.59	0.04 ± 0.03
15038+4739	0.78 ± 0.02	0.78 ± 0.27	0.79 ± 0.15
15183+2650	0.05 ± 0.01	0.27 ± 0.20	0.04 ± 0.01
15232+3017	0.29 ± 0.01	0.38 ± 0.20	0.25 ± 0.06
15427+2618	1.56 ± 0.01	2.34 ± 0.68	1.48 ± 0.07
16309+0159	1.04 ± 0.02	1.37 ± 0.54	1.01 ± 0.03
17104−1544	0.51 ± 0.01	0.46 ± 0.21	0.5
19307+2758	2.12 ± 0.02	1.97 ± 0.41	...
19553−0644	1.04 ± 0.05	0.99 ± 0.35	...
20035+3601	0.61 ± 0.01	0.50 ± 0.17	0.52 ± 0.00
20181+4044	2.27 ± 0.02	2.10 ± 0.27	2.25 ± 0.17
20203+3924	...	1.81 ± 0.55	...
20375+1436[a]	0.91 ± 0.05	0.91 ± 0.34	0.9 ± 0.3
21044−1951	2.37 ± 0.06	1.60 ± 0.43	1.67 ± 0.72
21145+1000	0.33 ± 0.32	0.16 ± 0.19	0.62 ± 0.31
21148+3803	2.89 ± 0.03	3.13 ± 0.79	2.46 ± 0.15
21186+1134	1.57 ± 0.25	1.69 ± 0.38	1.13 ± 0.46
21441+2845	1.45 ± 0.01	1.44 ± 0.29	1.47 ± 0.21
21501+1717	1.21 ± 0.31	1.06 ± 0.48	1.1
22300+0426	1.54 ± 0.01	1.40 ± 0.35	1.33 ± 0.12
22586+0921	...	0.24 ± 0.19	0.7

[a] Red Δm from SOR AO paper is 1.04 ± 0.01.

USNO is currently preparing a new WDS, which will include the Δm catalog and incorporate multidimensional weighting of data to provide a more accurate representation of Δm.[7]

Although not widely noted, many clever and useful approaches to measuring Δm's were developed prior to the modern generation of techniques based upon digital detectors. These methods generally provided measurements freer of subjective bias than simple visual estimates of Δm and include such techniques as double image photometry (Pickering 1879; Stebbins 1907; Wendell 1913), wedge photometry (Wallenquist 1947; Pettit 1958; Rakos et al. 1982), objective gratings (Baize 1950), double image micrometry (Muller 1952; van Herk 1966; Worley 1969), and area scanning (Rakos et al. 1982; O. G. Franz 1982, private communication).

The above methods are generally no longer practiced, and no methods of even comparable reliability have come along to replace them in any systematic fashion. Speckle interferometry offers the potential for extracting differential photometric information from speckle images, but the actual practice of this is not straightforward. In many cases, speckle data are obtained with nonlinear image intensifiers, often yielding saturated images. Calibration for atmospherically induced biases in speckle data is also a nontrivial task. Perhaps the best speckle photometric analysis is that of Bagnuolo & Sowell (1988) for the components of Capella. However, the overall brightness and near-zero Δm of that system make it an ideal candidate for careful speckle analysis. Dombrowski (1990) measured Δm's in V for Hyades binaries using the "fork" algorithm of Bagnuolo (1988) applied to speckle data and found $\Delta m = 0.19$ for WDS 04512+1104, in satisfactory agreement with our value of $\Delta m = 0.15 \pm 0.04$. Ismailov (1992) fitted visibility curves from speckle data obtained at 500 nm. Seven of our systems were also measured by Ismailov, and in comparing our results with his in the sense of AO minus speckle, we find a dispersion of ±0.76 mag, indicative of poor agreement with Ismailov's differential photometry.

[7] For further information, see http://aries.usno.navy.mil/ad/wds/wds.html.

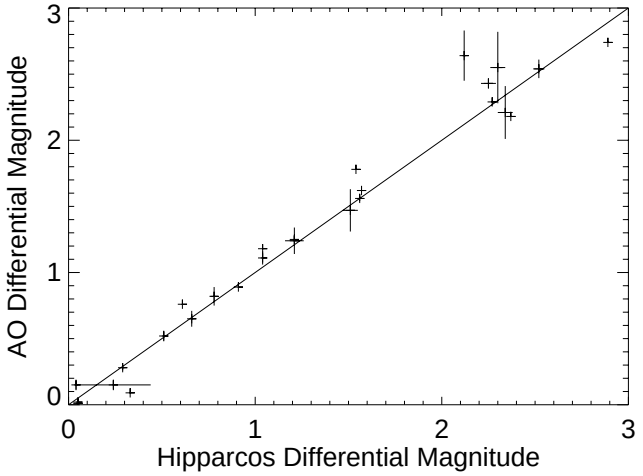

FIG. 1.—Comparison of *Hipparcos* measures of differential magnitude with the measures made on the Mount Wilson 100 inch AO system.

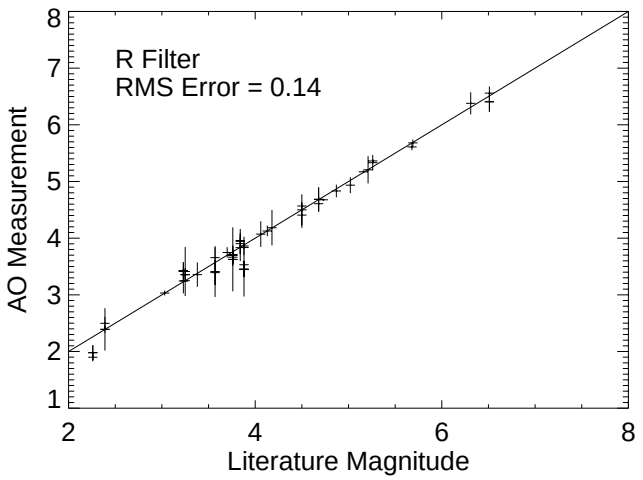

FIG. 2.—An example of the photometric results, with the total photometry as measured by the AO system compared with the values found in the literature.

The Δm measurements of *Hipparcos* are plotted against our V-band measurements in Figure 1. Even though the *Hipparcos* photometric band H_p is broader and peaks blueward in comparison with the standard Johnson V used with the Mount Wilson AO system, Figure 1 clearly shows that our measurements are consistent with those of *Hipparcos*, with the errors increasing with increasing Δm as one would expect. For small-Δm objects the match between our data and those of *Hipparcos* is excellent. From residuals defined in the sense AO minus *Hipparcos*, we find a mean residual and rms dispersion of $+0.03 \pm 0.15$ mag, improving to $+0.01 \pm 0.10$ mag when we omit systems for which we calculate $\Delta m \geq 2.0$. We find no obvious correlation between spectral type of the primary component and the AO $-$ *Hipparcos* residual, although most of our stars are confined to systems of intermediate spectral types. A similar comparison in AO-minus-WDS magnitudes yields a mean and standard deviation of $+0.06 \pm 0.35$ mag, with no significant improvement resulting from including only systems with smaller Δm's.

Another test of the accuracy of our AO photometry is obtained by comparing our new results with photometry from another AO system. Thus, we note that the R-band Δm for WDS 20375+1436 measured at SOR (ten Brummelaar et al. 1996) was 1.04 ± 0.01 while our new measurements on two nights at Mount Wilson are 0.93 ± 0.11 and 1.03 ± 0.08. As discussed above, we now believe that the errors given for the SOR measures are underestimated. Furthermore, the filters used at SOR were not standard astronomical filters. Nevertheless, the two measures at Mount Wilson are entirely consistent with the earlier SOR measurement. Unfortunately, this is the only system we have in

TABLE 4

COMPONENT APPARENT MAGNITUDES

WDS α, δ (2000)	B		V		R		I	
	Primary	Secondary	Primary	Secondary	Primary	Secondary	Primary	Secondary
00022+2705	...	...	5.81 ± 0.03	8.89 ± 0.29	5.25 ± 0.03	7.95 ± 0.27	4.85 ± 0.03	7.20 ± 0.26
00318+5431	...	...	5.41 ± 0.03	5.56 ± 0.05	5.43 ± 0.03	5.53 ± 0.05	5.54 ± 0.03	5.67 ± 0.05
02140+4729	...	...	6.54 ± 0.03	7.19 ± 0.07	6.18 ± 0.02	6.77 ± 0.05	5.95 ± 0.02	6.49 ± 0.03
04139+0916	...	...	4.95 ± 0.02	7.38 ± 0.04	4.26 ± 0.02	7.12 ± 0.07	3.78 ± 0.02	7.06 ± 0.13
04239+0928	...	...	5.51 ± 0.04	6.41 ± 0.13	5.39 ± 0.04	6.36 ± 0.12	5.62 ± 0.03	5.83 ± 0.05
04301+1538	...	...	5.70 ± 0.03	8.05 ± 0.20	5.40 ± 0.03	7.59 ± 0.17	5.23 ± 0.03	7.25 ± 0.12
	...	...	5.68 ± 0.02	8.22 ± 0.07	5.38 ± 0.02	7.75 ± 0.05	5.20 ± 0.02	7.41 ± 0.04
04382−1418	...	...	...	...	3.14 ± 0.03	5.53 ± 0.23	2.54 ± 0.02	5.56 ± 0.20
04512+1104	...	...	7.45 ± 0.03	7.60 ± 0.05	6.98 ± 0.03	7.16 ± 0.05	6.67 ± 0.03	6.87 ± 0.05
05387−0236	...	...	4.10 ± 0.03	5.34 ± 0.10	4.15 ± 0.04	5.49 ± 0.13	4.41 ± 0.04	5.66 ± 0.16
05413+1632	...	...	5.11 ± 0.04	6.58 ± 0.16	5.11 ± 0.04	6.62 ± 0.18	5.23 ± 0.04	6.75 ± 0.18
06573+5825	...	...	4.67 ± 0.03	5.83 ± 0.12	3.96 ± 0.03	5.37 ± 0.08	3.48 ± 0.04	5.08 ± 0.18
09006+4147	...	...	4.07 ± 0.03	6.62 ± 0.27	3.71 ± 0.03	5.90 ± 0.15	3.50 ± 0.04	5.56 ± 0.23
11182+3132	4.87 ± 0.04	5.49 ± 0.09	4.31 ± 0.04	4.84 ± 0.10	3.79 ± 0.03	4.26 ± 0.07	3.48 ± 0.03	3.88 ± 0.05
	4.92 ± 0.03	5.39 ± 0.06	4.35 ± 0.03	4.77 ± 0.07	3.87 ± 0.03	4.15 ± 0.07	3.58 ± 0.03	3.76 ± 0.05
13099−0532	4.54 ± 0.04	6.65 ± 0.23	4.52 ± 0.03	6.73 ± 0.20	4.48[a] ± 0.13	6.56[a] ± 0.24	4.11[a] ± 0.32	6.27[a] ± 0.38
13100+1732	5.50 ± 0.03	5.54 ± 0.05	5.08 ± 0.04	5.07 ± 0.07	4.83[a] ± 0.11	4.83[a] ± 0.12	4.21[a] ± 0.25	4.21[a] ± 0.25
14411+1344	4.58 ± 0.02	4.58 ± 0.03	4.52 ± 0.02	4.54 ± 0.02	4.51 ± 0.02	4.52 ± 0.02	4.51 ± 0.02	4.53 ± 0.02
	4.59 ± 0.05	4.57 ± 0.10	4.50 ± 0.03	4.57 ± 0.05	4.51 ± 0.02	4.52 ± 0.04	4.50 ± 0.02	4.55 ± 0.04
15038+4739	5.71 ± 0.04	6.99 ± 0.17	5.19 ± 0.03	6.01 ± 0.08	4.38[a] ± 0.14	4.99[a] ± 0.14	4.51[a] ± 0.32	5.03[a] ± 0.32
15183+2650	7.79 ± 0.03	7.81 ± 0.05	7.34 ± 0.02	7.35 ± 0.04	...	...	...	...
15232+3017	6.16 ± 0.02	6.48 ± 0.03	5.60 ± 0.02	5.88 ± 0.03	5.13 ± 0.02	5.39 ± 0.02	4.85 ± 0.02	5.10 ± 0.02
	7.64 ± 0.03	8.00 ± 0.07	7.21 ± 0.03	7.50 ± 0.07	...	...	...	...
15427+2618	4.05 ± 0.02	5.74 ± 0.08	4.08 ± 0.02	5.64 ± 0.03	4.14 ± 0.02	5.57 ± 0.03	4.18 ± 0.02	5.51 ± 0.04
	4.02 ± 0.03	5.87 ± 0.11	4.08 ± 0.03	5.67 ± 0.12	4.14 ± 0.02	5.55 ± 0.06	4.19 ± 0.02	5.47 ± 0.06
16309+0159	...	...	4.17 ± 0.04	5.24 ± 0.15	4.20 ± 0.02	5.23 ± 0.05	4.21 ± 0.02	5.23 ± 0.04
	4.17 ± 0.03	5.29 ± 0.08	4.16 ± 0.02	5.27 ± 0.06	4.18 ± 0.02	5.27 ± 0.06	4.20 ± 0.02	5.26 ± 0.04
17104−1544	3.00 ± 0.03	3.50 ± 0.07	2.94 ± 0.03	3.46 ± 0.05	2.91 ± 0.02	3.44 ± 0.04	2.90 ± 0.02	3.43 ± 0.03
.....	2.99 ± 0.04	3.53 ± 0.09	2.98 ± 0.03	3.40 ± 0.06	2.93 ± 0.02	3.40 ± 0.03	2.91 ± 0.02	3.40 ± 0.02
19307+2758	...	...	3.18 ± 0.03	5.82 ± 0.19	2.26 ± 0.02	5.73 ± 0.26	...	...
19553−0644	7.20 ± 0.03	8.42 ± 0.10	6.82 ± 0.04	8.00 ± 0.13	6.60[a] ± 0.14	7.70[a] ± 0.17	5.47[a] ± 0.32	6.63[a] ± 0.33
	7.51 ± 0.03	7.79 ± 0.07	6.90 ± 0.04	7.78 ± 0.13	6.62[a] ± 0.14	7.62[a] ± 0.18	5.47[a] ± 0.32	6.62[a] ± 0.35
20035+3601	7.16 ± 0.02	7.95 ± 0.05	7.07 ± 0.02	7.83 ± 0.03	6.95 ± 0.02	7.70 ± 0.02	6.84 ± 0.02	7.58 ± 0.02
20181+4044	6.03 ± 0.02	8.75 ± 0.07	5.96 ± 0.02	8.25 ± 0.04	5.81 ± 0.02	8.12 ± 0.03	5.80 ± 0.02	8.11 ± 0.02
20203+3924	6.44 ± 0.03	8.51 ± 0.22	6.40 ± 0.03	8.36 ± 0.18	6.33 ± 0.04	8.34 ± 0.22	6.35 ± 0.04	8.03 ± 0.19
20375+1436	4.37 ± 0.04	5.62 ± 0.15	4.03 ± 0.04	4.92 ± 0.12	3.61 ± 0.04	4.54 ± 0.12	3.33 ± 0.04	4.40 ± 0.15
	4.48 ± 0.03	5.32 ± 0.06	4.00 ± 0.03	4.97 ± 0.07	3.59 ± 0.03	4.62 ± 0.09	3.41 ± 0.03	4.24 ± 0.10
21044−1951	5.11 ± 0.03	7.78 ± 0.26	4.98 ± 0.03	7.16 ± 0.22	4.84 ± 0.03	6.87 ± 0.21	4.81 ± 0.04	6.53 ± 0.18
21145+1000	5.65 ± 0.03	5.84 ± 0.05	5.20 ± 0.03	5.29 ± 0.05	4.77 ± 0.03	4.86 ± 0.05	4.34 ± 0.03	4.77 ± 0.06
21148+3803	4.21 ± 0.03	7.01 ± 0.22	3.81 ± 0.02	6.55 ± 0.12	3.47 ± 0.02	6.09 ± 0.09	3.24 ± 0.02	5.83 ± 0.10
21186+1134	7.31 ± 0.04	8.99 ± 0.18	7.25 ± 0.03	8.87 ± 0.14	6.97[a] ± 0.13	8.50[a] ± 0.22	5.12[a] ± 0.25	6.69[a] ± 0.29
21441+2845	5.25 ± 0.02	6.72 ± 0.04	...	...	4.39 ± 0.02	5.80 ± 0.03	4.12 ± 0.02	5.50 ± 0.02
22300+0426	6.05 ± 0.04	8.06 ± 0.22	5.71 ± 0.04	7.49 ± 0.20	5.45 ± 0.04	6.99 ± 0.15	5.27 ± 0.03	6.69 ± 0.12

[a] Based on our photometry.

TABLE 5

COMPONENT COLORS

WDS α, δ (2000)	$B-V$		$V-R$		$V-I$	
	Primary	Secondary	Primary	Secondary	Primary	Secondary
00022+2705.....	...	...	0.57 ± 0.04	0.95 ± 0.40	0.96 ± 0.04	1.69 ± 0.39
00318+5431.....	...	...	−0.02 ± 0.04	0.03 ± 0.07	−0.13 ± 0.04	−0.11 ± 0.07
02140+4729.....	...	...	0.36 ± 0.04	0.42 ± 0.08	0.59 ± 0.04	0.70 ± 0.07
04139+0916.....	...	...	0.69 ± 0.03	0.26 ± 0.09	1.17 ± 0.03	0.32 ± 0.14
04239+0928.....	...	...	0.12 ± 0.06	0.05 ± 0.17	−0.11 ± 0.05	0.58 ± 0.14
04301+1538.....	...	...	0.30 ± 0.04	0.46 ± 0.27	0.47 ± 0.04	0.80 ± 0.24
	...	...	0.30 ± 0.03	0.47 ± 0.09	0.48 ± 0.03	0.81 ± 0.08
04512+1104.....	...	...	0.47 ± 0.04	0.44 ± 0.07	0.78 ± 0.04	0.73 ± 0.07
05387−0236.....	...	...	−0.05 ± 0.05	−0.15 ± 0.17	−0.31 ± 0.05	−0.32 ± 0.19
05413+1632.....	...	...	−0.00 ± 0.06	−0.04 ± 0.25	−0.12 ± 0.06	−0.17 ± 0.25
06573+5825.....	...	...	0.71 ± 0.04	0.46 ± 0.14	1.19 ± 0.05	0.75 ± 0.22
09006+4147.....	...	...	0.36 ± 0.04	0.72 ± 0.31	0.57 ± 0.05	1.06 ± 0.36
11182+3132.....	0.56 ± 0.05	0.65 ± 0.13	0.52 ± 0.05	0.58 ± 0.12	0.83 ± 0.05	0.96 ± 0.11
	0.57 ± 0.04	0.62 ± 0.09	0.48 ± 0.05	0.62 ± 0.10	0.78 ± 0.04	1.02 ± 0.08
13099−0532.....	0.01 ± 0.05	−0.09 ± 0.31	0.04 ± 0.14	0.17 ± 0.31	0.41 ± 0.32	0.46 ± 0.43
13100+1732.....	0.43 ± 0.05	0.48 ± 0.09	0.25 ± 0.12	0.24 ± 0.14	0.87 ± 0.25	0.86 ± 0.26
14411+1344.....	0.06 ± 0.03	0.04 ± 0.04	0.02 ± 0.03	0.03 ± 0.03	0.01 ± 0.03	0.01 ± 0.03
	0.09 ± 0.06	0.00 ± 0.11	−0.01 ± 0.04	0.05 ± 0.06	0.00 ± 0.04	0.02 ± 0.06
15038+4739.....	0.52 ± 0.05	0.98 ± 0.18	0.81 ± 0.14	1.02 ± 0.16	0.67 ± 0.32	0.97 ± 0.33
15183+2650.....	0.46 ± 0.04	0.47 ± 0.06	...	...	...	...
15232+3017.....	0.56 ± 0.03	0.60 ± 0.04	0.47 ± 0.03	0.49 ± 0.04	0.75 ± 0.03	0.78 ± 0.04
	0.43 ± 0.05	0.50 ± 0.10	...	...	...	...
15427+2618.....	−0.03 ± 0.03	0.10 ± 0.09	−0.06 ± 0.03	0.07 ± 0.04	−0.10 ± 0.03	0.13 ± 0.05
	−0.05 ± 0.04	0.21 ± 0.17	−0.07 ± 0.04	0.11 ± 0.14	−0.12 ± 0.04	0.19 ± 0.14
16309+0159.....	...	...	−0.02 ± 0.05	0.02 ± 0.15	−0.03 ± 0.05	0.02 ± 0.15
	0.01 ± 0.04	0.02 ± 0.09	−0.02 ± 0.03	0.00 ± 0.08	−0.03 ± 0.03	0.02 ± 0.07
17104−1544.....	0.06 ± 0.04	0.04 ± 0.08	0.03 ± 0.03	0.02 ± 0.06	0.04 ± 0.03	0.03 ± 0.06
	0.00 ± 0.05	0.12 ± 0.10	0.05 ± 0.04	−0.00 ± 0.06	0.07 ± 0.03	−0.00 ± 0.06
19307+2758.....	...	...	0.92 ± 0.03	0.09 ± 0.32	...	...
19553−0644.....	0.38 ± 0.05	0.42 ± 0.16	0.22 ± 0.15	0.30 ± 0.21	1.34 ± 0.32	1.36 ± 0.35
	0.61 ± 0.05	0.01 ± 0.14	0.28 ± 0.15	0.16 ± 0.22	1.43 ± 0.32	1.16 ± 0.37
20035+3601.....	0.09 ± 0.03	0.12 ± 0.05	0.12 ± 0.03	0.13 ± 0.04	0.22 ± 0.03	0.24 ± 0.04
20181+4044.....	0.06 ± 0.03	0.49 ± 0.09	0.15 ± 0.03	0.13 ± 0.05	0.16 ± 0.03	0.14 ± 0.05
20203+3924.....	0.05 ± 0.05	0.16 ± 0.29	0.07 ± 0.05	0.02 ± 0.29	0.05 ± 0.05	0.33 ± 0.27
20375+1436.....	0.34 ± 0.06	0.70 ± 0.19	0.41 ± 0.05	0.37 ± 0.16	0.69 ± 0.06	0.51 ± 0.19
	0.48 ± 0.04	0.35 ± 0.09	0.42 ± 0.04	0.36 ± 0.11	0.60 ± 0.04	0.74 ± 0.12
21044−1951.....	0.13 ± 0.04	0.62 ± 0.34	0.14 ± 0.05	0.29 ± 0.31	0.16 ± 0.05	0.62 ± 0.29
21145+1000.....	0.45 ± 0.04	0.55 ± 0.07	0.43 ± 0.04	0.43 ± 0.07	0.86 ± 0.04	0.52 ± 0.08
21148+3803.....	0.40 ± 0.03	0.46 ± 0.25	0.34 ± 0.03	0.46 ± 0.15	0.58 ± 0.03	0.73 ± 0.16
21186+1134.....	0.06 ± 0.05	0.12 ± 0.23	0.28 ± 0.14	0.37 ± 0.26	2.13 ± 0.25	2.18 ± 0.32
22300+0426.....	0.34 ± 0.05	0.57 ± 0.30	0.27 ± 0.05	0.51 ± 0.26	0.44 ± 0.05	0.80 ± 0.24

common with our earlier SOR results. Similarly, we note that the Δm at V of 1.67 ± 0.72 mag measured from lunar occultation data for WDS 21044−1951 by Evans & Edwards (1983) is within 1 standard deviation of our value of 2.18 ± 0.22.

As a final test, different measures of the same system on different nights, while of variable quality, show that the methodology used produces repeatable results. Nine systems in Table 2 were measured on successive nights. Inspection of the pairs of measurements of Δm in V, R, and I show mean dispersions of ±0.051, ±0.041, and ±0.046 mag at those passbands, respectively. These comparisons lend confidence in a level of precision of ±0.05 mag. Because we find no evidence for any systematic differences between our differential photometry and that from the *Hipparcos* mission, we suggest that this level of internal consistency is also indicative of the accuracy of our measurements.

3. ABSOLUTE PHOTOMETRY

Differential magnitudes must be combined with composite photometry of the system as a whole in order to obtain apparent magnitudes of the individual components, using the equations

$$m_A = m + 2.5 \log (1 + 10^{-0.4\Delta m}) , \quad (6)$$

$$m_B = m_A + \Delta m . \quad (7)$$

The General Catalogue of Photometric Data (Mermilliod, Mermilliod, & Hauck 1997)[8] provides a comprehensive listing of the composite photometric data on most of the systems we measured. Few of these records provided error estimates, so they were assumed to be ±0.02 mag in all cases. For the objects for which we could not find literature

[8] See http://obswww.unige.ch/gcpd/gcpd.html.

TABLE 6

COMPONENT ABSOLUTE MAGNITUDES

WDS α, δ (2000)	B		V		R		I	
	Primary	Secondary	Primary	Secondary	Primary	Secondary	Primary	Secondary
00022+2705	...	...	5.34 ± 0.09	8.42 ± 0.30	4.78 ± 0.09	7.48 ± 0.28	4.38 ± 0.09	6.73 ± 0.27
00318+5431	...	...	0.23 ± 0.25	0.38 ± 0.26	0.25 ± 0.25	0.35 ± 0.26	0.36 ± 0.25	0.49 ± 0.26
02140+4729	...	...	3.45 ± 0.09	4.10 ± 0.11	3.09 ± 0.09	3.68 ± 0.10	2.86 ± 0.09	3.40 ± 0.09
04139+0916	...	...	−0.33 ± 0.34	2.10 ± 0.35	−1.02 ± 0.34	1.84 ± 0.35	−1.50 ± 0.34	1.78 ± 0.37
04239+0928	...	...	0.09 ± 0.25	0.99 ± 0.28	−0.03 ± 0.25	0.94 ± 0.28	0.20 ± 0.25	0.41 ± 0.25
04301−1538	...	...	2.50 ± 0.12	4.85 ± 0.23	2.20 ± 0.12	4.39 ± 0.21	2.03 ± 0.12	4.05 ± 0.17
	...	...	2.48 ± 0.12	5.02 ± 0.14	2.18 ± 0.12	4.55 ± 0.13	2.00 ± 0.12	4.21 ± 0.12
04382−1418	...	...	...	...	0.51 ± 0.05	2.90 ± 0.23	−0.09 ± 0.05	2.93 ± 0.21
04512+1104	...	...	3.97 ± 0.13	4.12 ± 0.13	3.50 ± 0.13	3.68 ± 0.13	3.19 ± 0.13	3.39 ± 0.13
05387−0236	...	...	−3.63 ± 0.70	−2.39 ± 0.70	−3.58 ± 0.70	−2.24 ± 0.71	−3.32 ± 0.70	−2.07 ± 0.71
05413+1632	...	...	−1.69 ± 0.61	−0.22 ± 0.63	−1.69 ± 0.61	−0.18 ± 0.64	−1.57 ± 0.61	−0.05 ± 0.64
06573+5825	...	...	1.08 ± 0.09	2.24 ± 0.15	0.37 ± 0.09	1.78 ± 0.12	−0.11 ± 0.10	1.49 ± 0.20
09006+4147	...	...	2.99 ± 0.06	5.54 ± 0.27	2.63 ± 0.06	4.82 ± 0.16	2.42 ± 0.06	4.48 ± 0.23
11182+3132	3.79 ± 0.06	4.41 ± 0.10	3.23 ± 0.06	3.76 ± 0.11	2.71 ± 0.06	3.18 ± 0.08	2.40 ± 0.06	2.80 ± 0.07
13099−0532	−0.98 ± 0.31	1.13 ± 0.38	−1.00 ± 0.31	1.21 ± 0.37	−1.04 ± 0.33	1.04 ± 0.39	−1.41 ± 0.44	0.75 ± 0.49
13100+1732	4.72 ± 0.86	4.76 ± 0.86	4.30 ± 0.86	4.29 ± 0.86	4.05 ± 0.86	4.05 ± 0.87	3.43 ± 0.89	3.43 ± 0.89
14411+1344	0.86 ± 0.15	0.86 ± 0.15	0.80 ± 0.15	0.82 ± 0.15	0.79 ± 0.15	0.80 ± 0.15	0.79 ± 0.15	0.81 ± 0.15
	0.87 ± 0.16	0.85 ± 0.18	0.78 ± 0.15	0.85 ± 0.16	0.79 ± 0.15	0.80 ± 0.15	0.78 ± 0.15	0.83 ± 0.15
15038+4739	5.18 ± 0.05	6.46 ± 0.17	4.66 ± 0.04	5.48 ± 0.08	3.85 ± 0.14	4.46 ± 0.14	3.98 ± 0.32	4.50 ± 0.32
15183+2650	4.87 ± 0.11	4.89 ± 0.12	4.42 ± 0.11	4.43 ± 0.11	...	...	...	...
15232+3017	4.81 ± 0.05	5.13 ± 0.06	4.25 ± 0.05	4.53 ± 0.06	3.78 ± 0.05	4.04 ± 0.05	3.50 ± 0.05	3.75 ± 0.05
	6.29 ± 0.06	6.65 ± 0.09	5.86 ± 0.06	6.15 ± 0.09	...	...	...	...
15427+2618	0.81 ± 0.07	2.50 ± 0.10	0.84 ± 0.07	2.40 ± 0.07	0.90 ± 0.07	2.33 ± 0.07	0.94 ± 0.07	2.27 ± 0.08
	0.78 ± 0.07	2.63 ± 0.13	0.84 ± 0.07	2.43 ± 0.14	0.90 ± 0.07	2.31 ± 0.09	0.95 ± 0.07	2.23 ± 0.09
16309+0159	...	...	0.63 ± 0.15	1.70 ± 0.21	0.66 ± 0.15	1.69 ± 0.16	0.67 ± 0.15	1.69 ± 0.15
	0.63 ± 0.15	1.75 ± 0.17	0.62 ± 0.15	1.73 ± 0.16	0.64 ± 0.15	1.73 ± 0.16	0.66 ± 0.15	1.72 ± 0.15
17104+1544	0.94 ± 0.06	1.44 ± 0.08	0.88 ± 0.06	1.40 ± 0.07	0.85 ± 0.05	1.38 ± 0.06	0.84 ± 0.05	1.37 ± 0.06
	0.93 ± 0.06	1.47 ± 0.10	0.92 ± 0.06	1.34 ± 0.08	0.87 ± 0.05	1.34 ± 0.06	0.85 ± 0.05	1.34 ± 0.05
19307+2758	...	...	−2.18 ± 0.15	0.46 ± 0.24	−3.10 ± 0.15	0.37 ± 0.30	...	...
19553+0644	2.54 ± 0.22	3.76 ± 0.24	2.16 ± 0.22	3.34 ± 0.26	1.94 ± 0.26	3.04 ± 0.28	0.81 ± 0.39	1.97 ± 0.40
	2.85 ± 0.22	3.13 ± 0.23	2.24 ± 0.22	3.12 ± 0.26	1.96 ± 0.26	2.96 ± 0.28	0.81 ± 0.39	1.96 ± 0.41
20181+4044	−2.36 ± 0.63	0.36 ± 0.63	−2.43 ± 0.63	−0.14 ± 0.63	−2.58 ± 0.63	−0.27 ± 0.63	−2.59 ± 0.63	−0.28 ± 0.63
20203+3924	1.25 ± 0.20	3.32 ± 0.29	1.21 ± 0.20	3.17 ± 0.27	1.14 ± 0.20	3.15 ± 0.29	1.16 ± 0.20	2.84 ± 0.27
20375+1436	1.99 ± 0.07	3.24 ± 0.16	1.65 ± 0.07	2.54 ± 0.13	1.23 ± 0.07	2.16 ± 0.13	0.95 ± 0.07	2.02 ± 0.16
	2.10 ± 0.06	2.94 ± 0.08	1.62 ± 0.06	2.59 ± 0.09	1.21 ± 0.06	2.24 ± 0.11	1.03 ± 0.06	1.86 ± 0.12
21044−1951	1.68 ± 0.16	4.35 ± 0.30	1.55 ± 0.16	3.73 ± 0.27	1.41 ± 0.16	3.44 ± 0.26	1.38 ± 0.16	3.10 ± 0.24
21145+1000	4.32 ± 0.05	4.51 ± 0.06	3.87 ± 0.05	3.96 ± 0.06	3.44 ± 0.05	3.53 ± 0.06	3.01 ± 0.05	3.44 ± 0.07
21148+3803	2.61 ± 0.04	5.41 ± 0.22	2.21 ± 0.03	4.95 ± 0.12	1.87 ± 0.03	4.49 ± 0.09	1.64 ± 0.03	4.23 ± 0.10
21186+1134	3.79 ± 0.14	5.47 ± 0.22	3.73 ± 0.13	5.35 ± 0.19	3.45 ± 0.18	4.98 ± 0.26	1.60 ± 0.28	3.17 ± 0.32
21441+2845	3.50 ± 0.04	4.97 ± 0.05	...	...	2.64 ± 0.04	4.05 ± 0.05	2.37 ± 0.04	3.75 ± 0.04
22300+0426	2.55 ± 0.14	4.56 ± 0.26	2.21 ± 0.14	3.99 ± 0.24	1.95 ± 0.14	3.49 ± 0.20	1.77 ± 0.14	3.19 ± 0.18

values, we were forced to use our own data to provide combined magnitudes. The data were reprocessed using a shift-and-add routine that weighted each frame equally and normalized the intensities to a 1 s exposure. The total intensity of each system was then calibrated against the literature values to obtain combined magnitudes. Figure 2 is a plot of our calibrated measures of total magnitudes against the literature values in the R band. Other bands produced similar results, and our final apparent magnitude results are given in Table 4, with those based on our photometry noted. The systems in Table 4 are identified by their WDS coordinate in the first column. The remaining columns provide the deconvolved magnitudes of the components. These data allow us to calculate the colors presented in Table 5, in which the first column provides the WDS coordinate and the remaining columns present the colors ($B-V$, $V-R$, and $R-I$) for the components. Table 6 contains absolute magnitudes for the individual components based on parallax results from *Hipparcos* (ESA 1997) and the apparent magnitudes in Table 4. The column headings are self-evident.

4. SPECTRAL TYPES AND DERIVED PARAMETERS

With colors and absolute magnitudes, it is now possible to assign spectral types, effective temperatures, and absolute bolometric magnitudes to the individual components of the systems we have observed. These results are shown in Table 7. The first two columns of Table 7 give the WDS designation and the spectral type listed in the WDS. The third column gives the composite spectral types of Christy & Walker (1969), Edwards (1976), or both. The magnitudes from Table 6 were used to generate three colors, for which spectral types and ranges were calculated using the tables of Johnson (1966). These results are given in columns (4)–(6) of Table 7. In each case, the table appropriate for the luminosity class of the WDS type was used, except in the few cases where the color difference was outside the values covered by that table. These systems are marked by notes in

TABLE 7

NEWLY DETERMINED SPECTRAL TYPES

WDS α, δ (2000) (1)	WDS Type (2)	Other Type (3)	$B-V$ Type (4)	$V-R$ Type (5)	$V-I$ Type (6)	V_{abs} Type (7)	Assigned (8)
00022+2705	G2 V	G2 V + K6 V,[a]	...	G7 (3–9)	G8 (6–9)	G7 (6–7)	G7 (6–8)
		G3 V + K7 V[b]	...	K5 (4–5)	K5 (4–8)	K8 (7–M0)	K5 (4–6)
00318+5431	B9 V	B7.5 V + B8.5 V[a]	...	B9 (7–A0)	B8 (7–9)	B8 (6–A0)	B8 (7–9)
			...	A0 (B7–A3)	B8 (B6–A1)	B9 (9–A0)	B9 (B8–A0)
02140+4729	F4 V	F3 V + F6 V,[a]	...	F2 (0–8)	F2 (0–5)	F2 (1–2)	F2 (1–3)
		F1 V + F4 V[b]	...	F6 (3–G0)	F6 (5–9)	F8 (8–9)	F7 (6–8)
04139+0916	G5 III* + A7 V	...	...	G5 (4–8)	G5 (4–8)	K7 (4–M3)	G5 (4–8)
			...	A8 (6–F2)	A8 (4–F0)	A6 (4–9)	A8 (5–F0)
04239+0928	A3 V	A3 V + A4 V[b]	...	A3 (2–6)	B8 (7–9)	B9 (3–A0)	A0 (B7–A4)
			...	A1 (B0–F0)	F3 (A9–F7)	A1 (0–2)	A1 (B5–F5)
04301+1538	F0 V*	A8 V + G2 V[a]	...	F0 (A9–F1)	F0 (A9–F1)	A9 (6–F0)	F0 (A9–F1)
			...	F7 (4–9)	G0 (F7–G5)	G7 (6–8)	G0 (F7–G7)
04512+1104	F7 V + F7 V	F7 V + F7 V,[a]	...	F8 (6–G0)	F8 (7–G0)	F8 (8–8)	F8 (7–G0)
		F8 V + F8 V[b]	F7 (4–G0)	F7 (6–9)	F8 (7–9)	F7 (6–8)	...
05387−0236	O9.5 V	O9 V + B0.5 V[a]	...	B6 (2–9)	B2 (1–3)	B0 (O9–B1)	B3 (1–4)
			...	O9 (5–A0)	B2 (O4–B5)	B2 (1–3)	B2 (O9–B4)
05413+1632	B3 IV	B3 IV + B3 V,[a]	...	B9 (6–A1)	B8 (7–9)	B3 (2–5)	B8 (7–9)
		B3 V + B4 V[b]	...	B7 (O5–A7)	B7 (0–A2)	B8 (6–9)	B7 (2–9)
06573+5825[c]	G5 III	...	...	G8 (0–K0)	G8 (0–K0)	A7 (6–8)	G8 (0–K0)
			...	F8 (5–G2)	F8 (4–G2)	Off scale	F8 (5–G2)
09006+4147	F5 V	...	...	F3 (1–5)	F3 (1–4)	F1 (0–1)	F3 (1–4)
			...	K2 (F5–K5)	K0 (F7–K4)	G9 (6–K0)	K0 (F8–K4)
11182+3132	G0 V + G0 V	...	F9 (F8–G0)	F8 (F6–G0)	F9 (F8–G0)	F1 (0–2)	F9 (F8–G0)
			G2 (F7–G7)	G9 (2–K1)	G9 (8–K0)	F7 (6–8)	G9 (6–K1)
13099−0532	A IV	...	A0 (0–1)	A1 (B2–F0)	A9 (A2–F7)	B6 (5–7)	A0 (B9–A1)
			B8 (7–9)	A6 (O9.5–F8)	F0 (A0–G0)	B6 (5–7)	B8 (7–9)
13100+1732	F6 V	F5 V + F5 V[a]	F5 (3–6)	A8 (A4–F3)	G3 (F4–K1)	G0 (F5–G6)	F5 (3–6)
			F6 (4–9)	A8 (A3–F4)	G3 (F4–K1)	G0 (F6–G6)	F6 (4–9)
14411+1344	A2 V	A2 III + A2 III[a]	A2 (1–3)	A0 (B9–A1)	A0 (0–1)	A0 (0–0)	A0 (B9–A1)
			A1 (0–3)	A0 (B9–A1)	A0 (0–1)	A0 (0–0)	A0 (B9–A1)
15038+4739	G0 V	...	F7 (6–9)	K3 (1–5)	F6 (A8–G8)	G2 (2–2)	F7 (6–9)
			K3 (0–5)	K5 (4–7)	G8 (F0–K3)	G8 (4–9)	K4 (2–6)
15183+2650	G0 V	...	F6 (5–7)	...	...	G0 (F9–G1)	F6 (5–7)
			F6 (5–7)	...	...	G0 (F9–G1)	F6 (5–7)
15232+3017	G3 V	G1 V + G3 V[a]	F9 (8–G0)	F8 (A9–F1)	F8 (7–8)	F9 (9–G0)	F8 (7–9)
			G0 (F9–G3)	G0 (F7–G2)	F9 (8–G0)	G1 (0–2)	G0 (F9–G1)
15427+2618	B9 IV + A3 V	B9 IV + A3 V[a]	B9 (9–A0)	B6 (2–8)	B8 (8–9)	A1 (0–1)	B9 (8–A0)
			A3 (0–7)	A2 (0–4)	A3 (2–4)	A8 (7–F0)	A3 (2–4)
16309+0159	A0 V + A4 V	A0 V + A4 V[a]	A0 (0–1)	B8 (6–9)	A0 (B9–0)	A0 (0–0)	A0 (B9–A0)
			A1 (B9–A4)	B9 (3–A2)	A0 (B9–A2)	A4 (3–5)	A0 (B8–A2)
17104−1544	A2 IV	A1 V + A3 V[a]	A2 (1–3)	A0 (B9–A1)	A1 (0–2)	A1 (1–1)	A1 (0–2)
			A1 (B9–A4)	A0 (B7–A2)	A1 (A0–A2)	A2 (2–3)	A1 (0–2)
19307+2758[d,e]	K3 II + B0 V	...	...	K3 (3–3)	...	Off scale	K3 (3–3)
			...	A2 (O5–F5)	...	A0 (B9–A1)	B0 (0–0)
20035+3601[f]	O9.5 III	...	A3 (2–4)	A4 (2–5)	A5 (4–6)	...	A4 (3–5)
			A2 (1–3)	A5 (3–7)	A6 (3–7)	...	A4 (2–6)
20181+4044[g]	O9 V	...	A2 (1–3)	A5 (3–7)	A4 (2–5)	B2 (1–3)	A4 (2–6)
			F7 (4–G0)	A4 (2–7)	A3 (2–4)	B8 (7–A0)	A3 (2–7)
20203+1436	A0 IV	A1 V + F6 V,[a]	A2 (0–4)	A2 (0–4)	A1 (0–2)	A2 (1–3)	A2 (1–3)
		A0 V + F1 V[b]	A6 (B7–F5)	A0 (O–F1)	A9 (1–F3)	F1 (0–2)	A5 (B7–F3)
20375+1436	F5 IV	F5 III + F5 IV,[a]	F6 (5–6)	F6 (4–8)	F4 (3–5)	A4 (3–5)	F5 (4–6)
		F6 III + F6 IV[b]	F2 (A9–F5)	F2 (A9–F8)	F7 (4–G2)	A9 (8–F0)	F2 (A9–F4)
21044−1951	A5 V	...	A5 (3–6)	A4 (2–7)	A4 (2–5)	A3 (2–4)	A4 (3–5)
			G1 (F0–K3)	F0 (B8–G8)	F4 (A8–G5)	F2 (1–8)	F2 (A5–G0)
21145+1000	F5 V + G0 V	F7 V + F7 V[b]	F5 (4–6)	F6 (5–8)	G2 (0–5)	F6 (5–7)	F6 (5–7)
			F9 (7–G2)	F6 (2–G0)	F1 (0–3)	F8 (7–8)	F6 (2–G0)
21148+3803	F3 IV–V	F0 IV + G1 V,[a]	F4 (2–5)	F2 (0–3)	F3 (2–4)	A7 (5–8)	F3 (2–4)
		F2 IV + G0 V[b]	F6 (A8–G1)	F8 (0–G9)	F7 (2–G5)	G4 (2–5)	F7 (2–G0)
21186+1134[h]	G0 V	F7 V + G6 V[b]	A2 (0–5)	F0 (A4–F6)	M0 (K6–M1)	F7 (5–8)	G0 (F0–M0)
			A4 (B7–F2)	F3 (A3–K0)	M0 (K6–M1)	G6 (5–8)	G6 (A5–M0)

[a] Edwards 1976.
[b] Christy & Walker 1969.
[c] Object went beyond luminosity class III table, used supergiant table instead.
[d] Used luminosity class I table.
[e] Used WDS spectral type.
[f] No *Hipparcos* measurement.
[g] Our type not consistent with WDS.
[h] Inconsistent result, used WDS type instead.

TABLE 8

EFFECTIVE TEMPERATURES, BOLOMETRIC MAGNITUDES, AND MASSES

WDS α, δ (2000) (1)	Assigned Type (2)	$T_{\rm eff}$ (K) (3)	$M_{\rm bol}$ (4)	Orbital Mass Sum ($M_\odot$) (5)	Spectroscopic Mass Sum ($M_\odot$) (6)
00022+2705.....	G7 (6–8)	5637 ± 70	5.00 ± 0.11	1.49 ± 0.09	1.6
	K5 (4–6)	4350 ± 200	7.70 ± 0.32		
00318+5431.....	B8 (7–9)	11900 ± 750	−0.57 ± 0.29	...	8.0
	B9 (B8–A0)	10500 ± 750	−0.13 ± 0.28		
02140+4729.....	F2 (1–3)	6890 ± 100	3.34 ± 0.09	2.39 ± 0.26	2.7
	F7 (6–8)	6280 ± 70	3.95 ± 0.11		
04139+0916.....	G5 (4–8)	5150 ± 100	−0.67 ± 0.34	...	5.0
	A8 (5–F0)	7580 ± 300	2.00 ± 0.35		
04239+0928.....	A0 (B7–A4)	9520 ± 1200	−0.21 ± 0.33	4.68	6.2
	A1 (B5–F5)	9230 ± 2240	0.76 ± 0.46		
04301+1538.....	F0 (A9–F1)	7200 ± 150	2.39 ± 0.12	2.56	2.8
	G0 (F7–G7)	5850 ± 600	4.82 ± 0.17		
04512+1104.....	F8 (7–G0)	6200 ± 40	3.81 ± 0.13	3.04 ± 0.49	2.4
	F7 (6–8)	6280 ± 40	3.97 ± 0.13		
05387−0236.....	B3 (1–4)	18700 ± 1500	−5.57 ± 0.73	...	21[a]
	B2 (O9–B4)	22000 ± 4000	−4.74 ± 0.81		
05413+1632.....	B8 (7–9)	11900 ± 625	−2.20 ± 0.62	...	9.1
	B7 (2–9)	13000 ± 2800	−1.24 ± 0.77		
06573+5825.....	G8 (0–K0)	4900 ± 275	0.66 ± 0.11	3.65 ± 1.83	4.1
	F8 (5–G2)	6100 ± 400	2.15 ± 0.16		
09006+4147.....	F3 (1–4)	6740 ± 100	2.87 ± 0.06	2.42 ± 0.12	2.2
	K0 (F8–K4)	5250 ± 400	5.23 ± 0.29		
11182+3132.....	F9 (F8–G0)	6220 ± 43	3.06 ± 0.06	2.21	1.9
	G9 (6–K1)	5410 ± 110	3.40 ± 0.11		
13099−0532.....	A0 (B9–A1)	9520 ± 317	−1.30 ± 0.32	...	7.5
	B8 (7–9)	11900 ± 650	0.41 ± 0.39		
13100+1732.....	F5 (3–6)	6440 ± 86	4.16 ± 0.86	2.54 ± 0.20	2.5
	F6 (4–9)	6378 ± 140	4.14 ± 0.86		
14411+1344.....	A0 (B9–A1)	10100 ± 380	0.40 ± 0.18	2.34	...
	A0 (B9–A1)	10100 ± 380	0.40 ± 0.18		
15038+4739.....	F7 (6–9)	6280 ± 60	4.51 ± 0.04	2.70 ± 0.16	1.9[a]
	K4 (2–6)	4590 ± 95	4.76 ± 0.14		
15183+2650.....	F6 (5–7)	6360 ± 40	4.27 ± 0.11	2.53 ± 0.33	2.5[a]
	F6 (5–7)	6360 ± 40	4.28 ± 0.11		
15232+3017.....	F8 (7–9)	6200 ± 40	4.09 ± 0.05	2.43	2.3
	G0 (F9–G1)	6030 ± 43	4.35 ± 0.06		
15427+2618.....	B9 (8–A0)	10500 ± 245	0.33 ± 0.14	4.23 ± 0.55	6.2
	A3 (2–4)	8720 ± 120	2.23 ± 0.07		
16309+0159.....	A0 (B9–A0)	9520 ± 70	0.32 ± 0.15	7.15	6.5
	A0 (B8–A2)	9520 ± 730	1.43 ± 0.22		
17104−1544.....	A1 (0–2)	9230 ± 130	0.65 ± 0.26	4.81 ± 3.31	5.5
	A1 (0–2)	9230 ± 130	0.65 ± 0.26		
19307+2758.....	K3 (3–3)	4080 ± 10	−2.93 ± 0.15	...	23
	B0 (0–0)	30000 ± 100	−2.70 ± 0.24		
20035+3601.....	A4 (3–5)	8460 ± 130	...	...	[a]
	A4 (2–6)	8460 ± 250	...		
20181+4044.....	A4 (2–6)	8460 ± 250	−2.59 ± 0.63	...	[a]
	A3 (2–7)	8720 ± 280	−0.31 ± 0.63		
20203+1436.....	A2 (1–3)	8970 ± 120	1.01 ± 0.20	1.56	4.8
	A5 (B7–F3)	8200 ± 1700	−0.29 ± 0.67		
20375+1436.....	F5 (4–6)	6440 ± 60	1.48 ± 0.06	3.34 ± 0.27	3.8
	F2 (A9–F4)	6890 ± 370	2.48 ± 0.09		
21044−1951.....	A4 (3–5)	8460 ± 130	1.39 ± 0.16	2.87 ± 0.75	3.8
	F2 (A5–G0)	6890 ± 540	3.62 ± 0.27		
21145+1000.....	F6 (5–7)	6360 ± 40	3.72 ± 0.05	2.35 ± 0.12	2.5
	F6 (2–G0)	6360 ± 215	3.81 ± 0.06		
21148+3803.....	F3 (2–4)	6740 ± 75	2.09 ± 0.03	2.71 ± 0.11	2.7
	F7 (2–G0)	6280 ± 210	4.80 ± 0.12		
21186+1134.....	G0 (F0–M0)	6030 ± 840	3.55 ± 0.35	3.07 ± 0.55	2.0[a]
	G6 (A5–M0)	5703 ± 1090	5.08 ± 0.36		

[a] Thought or known to be at least triple in multiplicity.

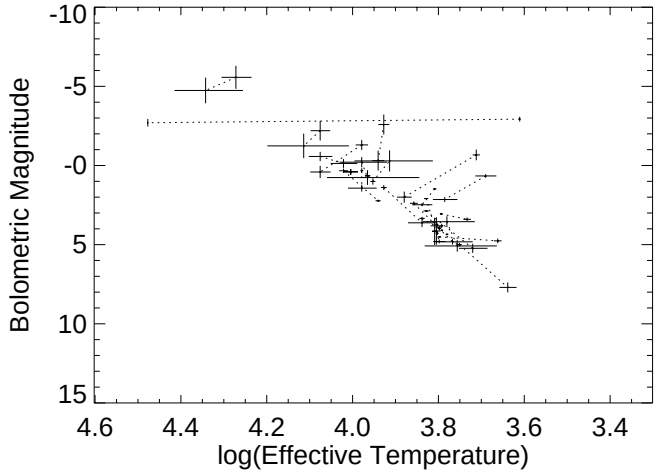

FIG. 3.—H-R diagram of all systems measured. The dotted lines connect primary and secondary on each system.

Table 7. A fourth measure of the spectral type, listed in column (7), was obtained by using the absolute magnitude from Table 6 and the tables of stellar temperatures and luminosity compiled by Schmidt-Kaler (1982). The final assignment and range of spectral type were given to each object by an averaging process, with the most weight being given to those measurements with color differences with the smallest range, and the least weight being given to the estimate based on absolute magnitude. The assigned spectral types resulting from our data are given in the last column of Table 7.

In most cases, especially those with the best color determinations, all four spectral type derivations yielded very consistent results. For those systems that did not have self-consistent results, either the error bars on the color differences were large, or the system is not a simple binary.

When we compare our spectral types with those listed in the second and third columns of Table 7, we find no evidence of any systematic differences and find an rms dispersion of approximately 2.3 subclasses in comparing our results with those taken from the literature. We exclude the two late O-type systems WDS 20035+3601 and WDS 20181+4044 in this evaluation, noting that these systems are known to have a third component not resolved in our measurements.

We used the assigned spectral types from Table 7 to derive astrophysical parameters for the individual components, which we present in Table 8. We repeat the WDS designation and assigned spectral type in the first two columns of Table 8. Column (3) contains $T_{\rm eff}$ values from Schmidt-Kaler (1982) corresponding to our spectral types, with errors based upon the range in the assigned type. Bolometric corrections taken from the same source were then used to calculate absolute bolometric magnitudes (using our absolute magnitudes in Table 6), which are recorded in column (4).

We also include in Table 8 information about the total mass for most of the systems we have observed. Söderhjelm (1999) calculated systemic masses for binaries for which reliable parallaxes were determined by *Hipparcos*, and we include his results for 15 systems in column (5) of Table 8. He calculated formal errors incorporating parallax error and uncertainties in the values of the orbital period and semimajor axis, and we include his error estimates in column (5). We have calculated mass sums for seven additional systems not considered by Söderhjelm but similarly based upon *Hipparcos* parallaxes and published orbital elements. We have not calculated error estimates for these mass sums, because the adopted orbits we have taken from the literature did not present formal errors for the elements P and a. Thus our "orbital" mass estimates in Table 8 are distinct from those of Söderhjelm (who calculated orbital elements himself directly from published visual or speckle observations) in the absence of error estimates. The final column in Table 8 gives an estimate of the total mass based upon the spectral types we have assigned to the individual components. The corresponding masses are taken from the tables of Allen (1973). We note those systems thought or known to be at least triple in multiplicity. In general, there are no surprises resulting from a comparison of the "orbital" and "spectroscopic" masses.

Given the effective temperatures and bolometric magnitudes, it is possible to plot the systems on the H-R diagram of Figure 3, in which the primary and secondary of each system are joined by a dotted line and error bars are shown for each component. As one might expect from our inherent sensitivity to modest Δm's, in most systems the primary and secondary do not fall very far apart on the H-R diagram, as a result of coevolutionary origins. Four systems exhibit post–main-sequence evolution of the more massive component. For one of these, WDS 19307+2758, our data were very poor. The $V-R$ type did not differ very much from the WDS designation, and the V designations were off scale. We therefore chose to accept the WDS types for the components, so this is not a new result. The other three, WDS 04139+0916, 06573+5825, and 20181+4044, have one component on the main sequence and the other component highly evolved.

5. CONCLUSION

Magnitudes and colors have been presented for the components of 36 binary star systems. Comparison with Δm measurements from the literature and examination of the H-R diagram and spectroscopic masses for these components demonstrates the reliability and self-consistency of these results. Thus, despite our early misgivings about the precision of adaptive optics measurements of close binaries, we have shown that it is possible to obtain good photometric results with an AO system. Four systems among those presented here appear to contain a highly evolved companion and deserve follow-up observation. Spectrographic data on these systems will be obtained in the near future in order to try to confirm these findings. Now that the reduction techniques have been developed, we hope that similar measurements will continue to be made, and we note the potentially valuable contribution AO observations can make when applied to systems with an intrinsically variable component.

We thank the staff of the Mount Wilson Institute for their help in making this work possible. CHARA's adaptive optics research has been supported by the National Science Foundation, most recently through grants AST 94-21259 and 94-23744, the Mount Wilson Institute, and the Research Program Enhancement fund at Georgia State University. Research with the adaptive optics system on Mount Wilson has also been supported by the Max Kampelman Fellowship fund, the Ahmanson Foundation, the Fletcher Jones Foundation, and the Parsons Foundation.

REFERENCES

Allen, C. W. 1973, Astrophysical Quantities (3d ed.; London: Athlone)
Bagnuolo, W. G. 1988, Opt. Lett., 13, 907
Bagnuolo, W. G., Jr., Mason, B. D., Barry, D. J., Hartkopf, W. I., & McAlister, H. A. 1992, AJ, 103, 1399
Bagnuolo, W. G., Jr., & Sowell, J. R. 1988, AJ, 96, 1056
Baize, P. 1950, J. Obs., 33, 1
———. 1980, A&AS, 39, 83
———. 1993, A&AS, 99, 205
Cester, B. 1991, Circ. d'Inf., No. 113
Christy, J. W., & Walker, R. L., Jr. 1969, PASP, 81, 643
Docobo, J. A., & Costa, J. A. 1987, Circ. d'Inf., No. 102
Docobo, J. A., & Ling, J. F. 1997, Circ. d'Inf., No. 133
———. 1999, ApJS, 120, 41
Dombrowski, E. G. 1990, Ph.D. thesis, Georgia State Univ.
Edwards, T. W. 1976, AJ, 81, 245
ESA. 1997, The Hipparcos and Tycho Catalogues (ESA SP-1200) (Noordwijk: ESA)
Evans, D. S., & Edwards, D. A. 1983, AJ, 88, 1845
Fekel, F. C., Scarfe, C. D., Barlow, D. J., Duquennoy, A., McAlister, H. A., Hartkopf, W. I., Mason, B. D., & Tokovinin, A. A. 1997, AJ, 113, 1095
Finsen, W. S. 1956, Union Obs. Circ., 6, 259
Finzi, C., & Giannuzzi, M. 1955, Oss. Astron. Roma Monte Mario Contrib. Sci., No. 222
Hall, R. G., Jr. 1949, AJ, 54, 102
Hartkopf, W. I., et al. 2000, AJ, in press
Hartkopf, W. I., Mason, B. D., & McAlister, H. A. 1996, AJ, 111, 370
Hartkopf, W. I., McAlister, H. A., & Franz, O. G. 1989, AJ, 98, 1014
Heintz, W. D. 1965, Veröff. Sternw. München, 7, No. 7
———. 1969, AJ, 74, 768
———. 1970, AJ, 75, 848
———. 1984, A&AS, 56, 5
———. 1995, ApJS, 99, 693
———. 1997, ApJS, 111, 335
Ismailov, R. M. 1992, A&AS, 96, 375
Johnson, H. L. 1966, ARA&A, 4, 193
Johnson, H. L., Mitchell, R. I., Iriarte, B., & Wisniewski, W. Z. 1966, Commun. Lunar Planet. Lab., 4, 99
Mason, B. D., Douglass, G. G., & Hartkopf, W. I. 1999, AJ, 117, 1023
Mason, B. D. McAlister, H. A., Hartkopf, W. I., & Shara, M. M. 1995, AJ, 109, 332
Mermilliod, J.-C., Mermilliod, M., & Hauck, B. 1997, A&AS, 124, 349
Muller, P. 1952, Ann. Obs. Strasbourg, 5, No. 4
Pettit, E. 1958, AJ, 63, 324
Pickering, E. 1879, Ann. Astron. Obs. Harvard Coll., 11, 105
Rakos, K., et al. 1982, A&As, 47, 221
Roberts, L. C., Jr. 1998, Ph.D. thesis, Georgia State Univ.
Schmidt-Kaler, T. 1982, in Landolt-Börnstein New Series, Group 6, Vol. 2b, Stars and Star Clusters, ed. K. Schaifers & H.-H. Voigt (Berlin: Springer), 1
Shelton, J. C., Schneider, T., McKenna, D., & Baliunas, S. L. 1995, Proc. SPIE, 2534, 72
Söderhjelm, S. 1999, A&A, 341, 121
Starikova, G. A. 1985, Tr. Gos. Astron. Inst. Shternberga, 57, 243
Stebbins, J. 1907, Univ. Illinois Stud., 2, No. 5
ten Brummelaar, T. A., Hartkopf, W. I., McAlister, H. A., Mason, B. D., Roberts, L. C., & Turner, N. H. 1998, Proc. SPIE, 3353, 391
ten Brummelaar, T. A., Mason, B. D. Bagnuolo, W. G., Jr., Hartkopf, W. I., McAlister, H. A., & Turner, N. H. 1996, AJ, 112, 1180
van Herk, G. 1966, J. Obs., 49, 355
Wallenquist, A. 1947, Uppsala Astron. Obs. Ann., 2, No. 2
Wendell, O. C. 1913, Ann. Astron. Obs. Harvard College, 69, 180
Wierzbinski, S. 1956, Acta Astron., 6, 82
Worley, C. E. 1969, AJ, 74, 764
Worley, C. E., & Douglass, G. G. 1997, A&AS, 125, 523
Zulević, D. J. 1988, Circ. d'Inf., No. 106